EurJIC European Journal of Inorganic Chemistry

ChemPubSoc Europe

FULL PAPER

DOI:10.1002/ejic.201402819

Synthesis and Biological Activity of Gold(I) N-Heterocyclic Carbene Complexes with Long Aliphatic Side Chains

Julià Arcau,[a] Vincent Andermark,[b] Mafalda Rodrigues,[c] Ilaria Giannicchi,[d] Lluïsa Pérez-Garcia,[c] Ingo Ott,[b] and Laura Rodríguez*[a]

Keywords: Carbene ligands / Gold / Imidazolium salts / Cytotoxicity / Enzyme inhibition

Seven imidazolium salts have been synthesized from octadecylimidazole (Im18). These salts differ in the length of the alkyl chain length bound to the second nitrogen atom of the imidazolium ring [R = Me, Et, *i*Pr, Pr, Bu, decyl (Dec), octadecyl] and were used as synthetic precursors to obtain two series of gold(I) carbene complexes (AuNHC). The first series contains one labile ligand at the second coordinative position {monocarbene, [AuCl(NHC)]}, and the second one comprises dicarbene complexes. Their biological activity has been evaluated with respect to two different cell lines, and thioredoxin reductase (TrxR) inhibition has also been evaluated for selected examples. Distinct effects have been observed for the imidazolium salts and monocarbene derivatives.

Introduction

Gold(I) N-heterocyclic carbene (Au^I–NHC) complexes have been known for more than a quarter of a century,[1] but their intensive study began only recently.[2–4]

The synthesis and characterization of new imidazolium salts[5] and NHC gold complexes have undergone rapid development in the past two decades, and their applications in medicine,[6–12] optics,[13–18] and a wide variety of catalytic processes[19–23] have been fascinating.

In particular, their use as anticancer agents has increased in recent years and they provide an alternative to cisplatin, which frequently presents associated drawbacks including severe normal tissue toxicity and resistance to treatment.[24] Thus, a number of structurally diverse gold(I) and gold(III) compounds have been prepared, such as those stabilized by phosphine or nitrogen atoms as donor groups, and they induce important anticancer effects both in vitro and in vivo.

The application of Au^I–NHC complexes for targeting mitochondrial cell death pathways was widely studied following the successful application of gold phosphine complexes as antitumor agents.[9,25]

An important aspect that regulates the biological activity of these organometallic complexes is the presence of an ancillary ligand coordinated to the gold center in addition to the NHC.[26]

Among the reported biologically active gold NHC complexes, distinct effects related to tumor cell proliferation inhibition have been described, including the increased formation of reactive oxygen species (ROS) or apoptosis induction.[26,27] However, it should be noted that a general direct correlation between thioredoxin reductase (TrxR) inhibition and the cytotoxic effects of gold NHC complexes has not always been observed;[28] this indicates that other mechanisms besides TrxR inhibition might contribute to the biological profile (e.g., interactions with G-quadruplexes).[28–30] Nevertheless, it was hypothesized that such strong inhibition of TrxR activity by gold complexes might result in a profound alteration of the mitochondrial membrane potential and ultimately lead to apoptotic cell death through activation of the mitochondrial pathway.[31–33] Moreover, it should be considered that TrxR is a ubiquitous flavoprotein that controls the regeneration of the functionality of small molecules (e.g., thioredoxin and glutathione), which are oxidized by different xenobiotics or enzymes belonging to the antioxidant network, and is responsible for controlling the cellular redox homeostasis. Consequently

[a] Departament de Química Inorgànica, Universitat de Barcelona, Martí i Franquès, 1-11, 08028 Barcelona, Spain
E-mail: laura.rodriguez@qi.ub.es
http://www.ub.edu/inorgani/en/index.html
[b] Institute of Medicinal and Pharmaceutical Chemistry, Technische Universität Braunschweig, Beethovenstr. 55, 38106 Braunschweig
[c] Laboratori de Química Orgànica, Facultat de Farmàcia, and Institut de Nanociència i Nanotecnologia (IN2UB), Universitat de Barcelona, 08028 Barcelona, Catalonia, Spain
[d] Dipartimento di Chimica and IMC-CNR Sezione Meccanismi di Reazione, Università La Sapienza, Box 34 Roma 62, 00185 Roma, Italy

Supporting information for this article is available on the WWW under http://dx.doi.org/10.1002/ejic.201402819.

the selective inhibition of this key enzyme represents a valuable parameter for the development of new gold-based anticancer drugs.[28]

In this work, we have synthesized a series of imidazolium salts from 1-octadecylimidazole by anchoring different alkyl groups (methyl, ethyl, isopropyl, propyl, butyl, decyl, and octadecyl) at the second nitrogen atom. The constant presence of an octadecylimidazole group on one side of the structure was chosen to facilitate cellular uptake. Moreover, we considered previous experiments with this imidazolium salt that provided interesting pharmacological results.[5]

Two different series of gold(I) carbene complexes (monocarbene and dicarbene) have been synthesized, and their biological activity was evaluated to analyze how the second alkyl chain length can affect the lipophilicity of the complex and the corresponding cytotoxicity and inhibition of the thioredoxin reductase enzyme.

Results and Discussion

Synthesis of Imidazolium Salts

Seven different imidazolium salts that differ in the alkyl chain length attached to one of the nitrogen atoms were synthesized by slight modifications of a previously reported experimental method.[34] The method is based on the reaction of octadecylimidazole (Im18) with the corresponding iodoalkane in acetonitrile (Scheme 1). The reaction solutions were stirred at 80 °C for ca. 20 h, and the products were generally obtained in high yields (70–90%) after concentration of the solution and the addition of diethyl ether.

The compounds were characterized by ^{1}H NMR and IR spectroscopy and mass spectrometry. The main evidence of the correct formation of the imidazolium salts is that the ^{1}H NMR resonance of the proton at the 2-position (between the two nitrogen atoms, see Figure 1) is downfield shifted by ca. 3 ppm after quaternization of the second nitrogen atom. Moreover, characteristic trends in the shift of 2-H, 4-H, and 5-H have been observed as the length of second alkyl chain increases (Figure 1). The proton at the 2-position shifts downfield by ca. 0.1–0.2 ppm as the alkyl chain length increases. On the other hand, 4-H and 5-H, which appear as two doublets for Im18, shift downfield by ca. 0.2 ppm after the formation of the 1-methyl-, 1-ethyl-, and 1-isopropyl-3-octadecylimidazolium salts. The ^{1}H NMR spectrum of **5** is almost identical to that corresponding to bis-Im18, as the chemical environment is quite similar at longer alkyl chain. Moreover, the chemical shifts of 4-H and 5-H overlap as the chain length increases [from the 1-butyl-3-octadecylimidazolium salt (**4**) and longer]. As expected, all methylene protons appear at upfield reso-

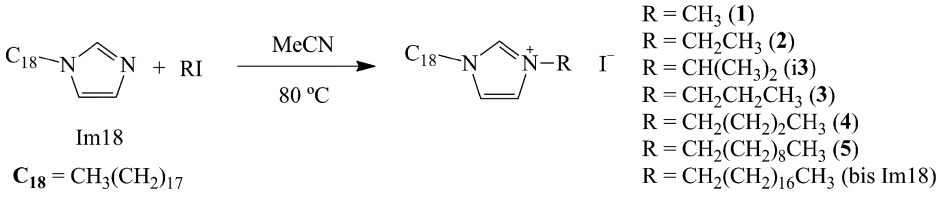

Scheme 1. Synthesis of the imidazolium salts used in this work.

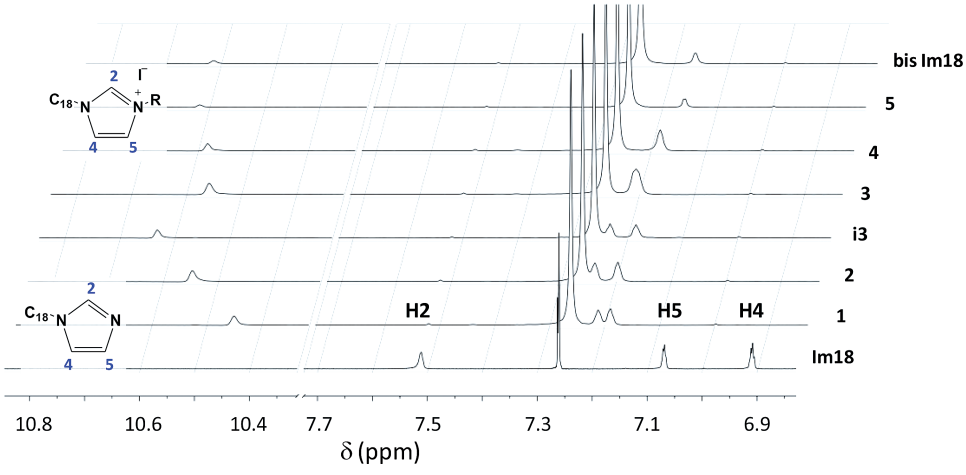

Figure 1. ^{1}H NMR spectra of the downfield resonance region of the different imidazolium salts.

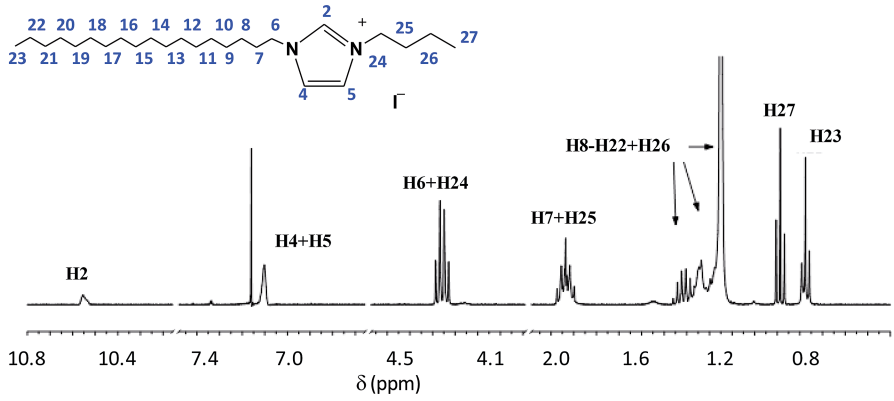

Figure 2. ^{1}H NMR spectrum of the upfield resonance region of the imidazolium salt **4** as an example.

nances (between δ = 4.5 and 0.5 ppm), as shown by the example spectrum in Figure 2.

The successful formation of the imidazolium salts was verified by ESI(+) MS, and the spectra showed the molecular peak for all compounds.

Synthesis of Monocarbene–Gold(I) Complexes

Six different complexes with the general structure [AuCl(NHC)] were synthesized by an established procedure (see Scheme 2).[35]

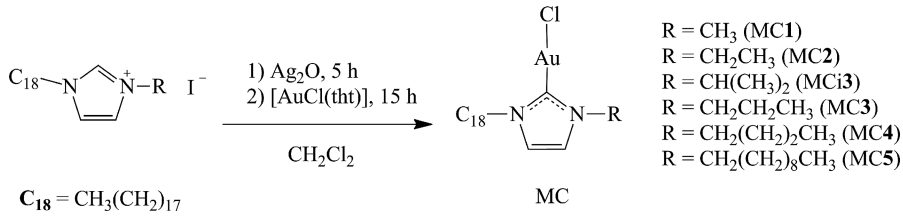

Scheme 2. Synthesis of monocarbene–gold(I) complexes.

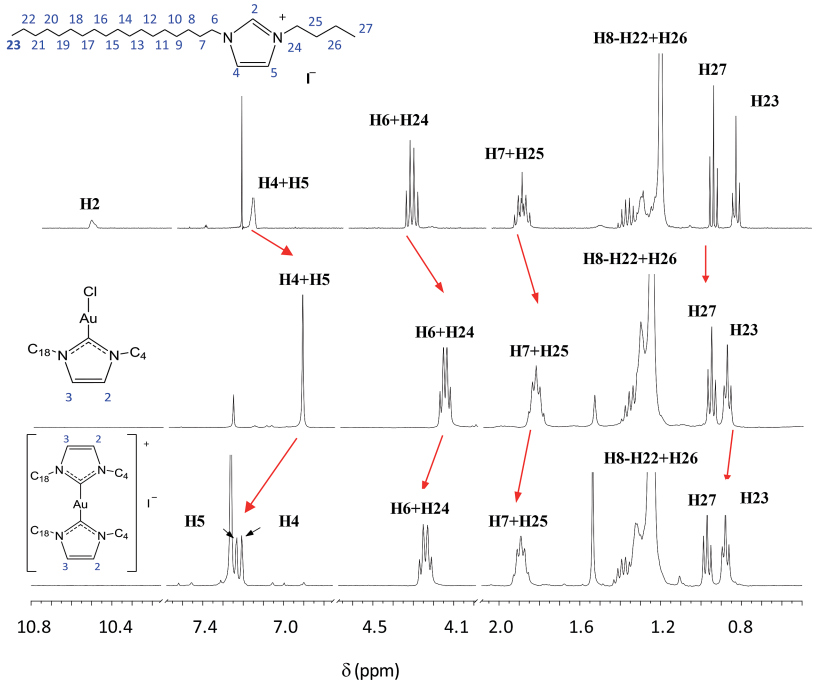

Figure 3. ^{1}H NMR spectra of the imidazolium salt **4**, the corresponding monocarbene MC**4**, and dicarbene DC**4**.

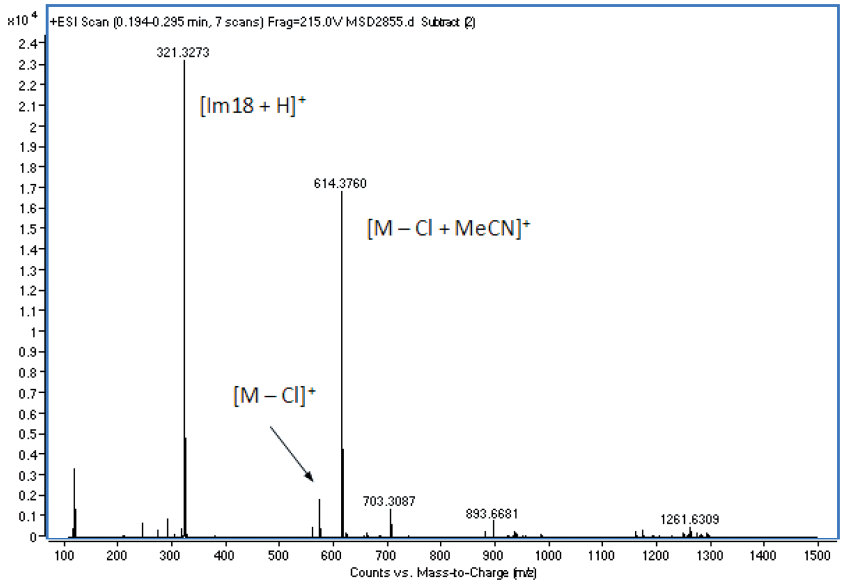

Figure 4. ESI(+) MS spectrum of MC**4**.

The resulting monocarbene complexes are solid-like complexes for shorter R groups (MC**1**–MC**4**), but they become oily for longer chain lengths, and a further purification process is needed to obtain them in pure form (recrystallization with CH_2Cl_2/hexane or column chromatography).

Characterization of the complexes by ^{1}H NMR and IR spectroscopy and ESI(+) mass spectrometry indicates their successful formation. As expected, the ^{1}H NMR spectra show the absence of the H-2 resonance that is characteristic of imidazolium salts. Moreover, as exemplified in Figure 3 for MC**4** and corresponding ligand **4**, the protons closer to the coordination position of the metal atom (H-2 to H-5, H-24, and H-25) are upfield-shifted by 0.2–0.3 ppm upon formation of the carbene derivatives. As previously observed for imidazolium salts **1**–**5**, H-4 and H-5 are observed as two doublets, but only a singlet is observed when the chemical environment becomes similar (longer alkyl chains, Figures S1–S2).

The IR spectra also indicate coordination of the gold(I) atom, as shown in the shift of the bands to higher wavenumbers by ca. 20 cm^{-1}. Moreover, the ESI(+) MS spectra show $[M - Cl]^+$ and $[M - Cl + MeCN]^+$ peaks in all cases, as exemplified in Figure 4 for MC**4**.

Synthesis of Dicarbene–Gold(I) Derivatives

The synthesis of the dicarbene gold(I) complexes was performed by a previously reported method with slight modifications (see Scheme 3).[35]

Characterization by ^{1}H NMR spectroscopy indicates that the chemical shifts are between those recorded for imidazolium salts **1**–**5** and the respective [AuCl(NHC)] complexes MC**1**–MC**5** (Figure 3). Moreover, from a detailed study of Figure 3, it can be observed that the equivalence of H-4 and H-5 in **4** and MC**4** is lost for the shorter alkyl chain compounds DC**1** and DC**4**. This could be because the most-stable conformation expected for asymmetric dicarbene complexes displays an *anti*-disposition of both ligands, as observed in X-ray crystal structures of dicarbene complexes.[36–38] The presence of a symmetrical carbene ligand precludes this *anti* conformation and is in agreement with the equivalence of these protons in DC**5** (Figures S3 and S4).

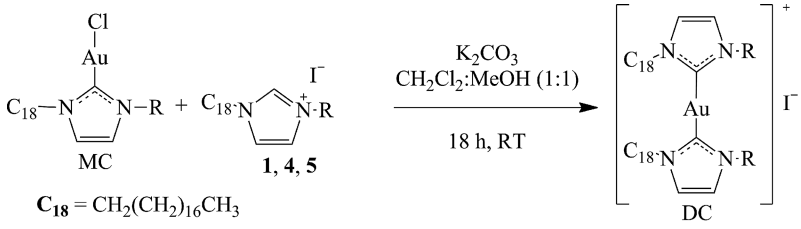

Scheme 3. Synthesis of dicarbene–gold(I) complexes.

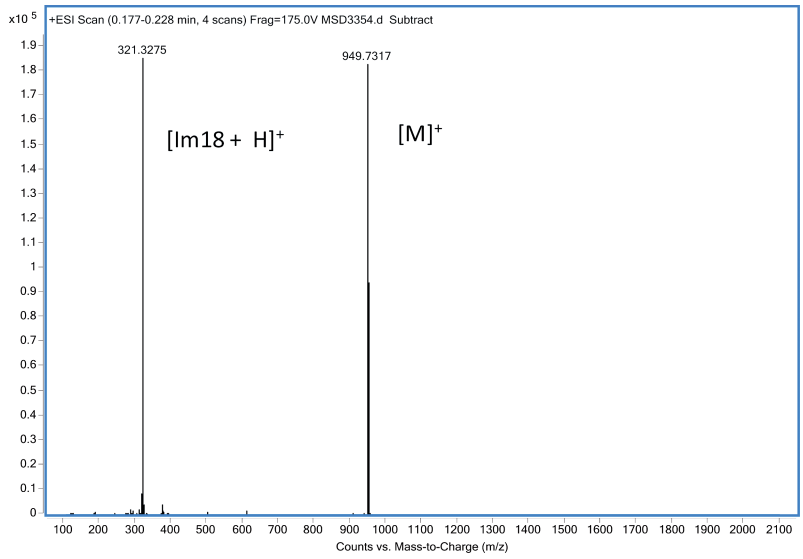

Figure 5. ESI(+) MS spectrum of DC**4**.

The ESI(+) MS spectra also display the corresponding molecular peaks for all complexes, as exemplified in Figure 5. Moreover, ESI(–) MS allowed us to identify that the counteranion is an iodide ion instead of the possible involvement of a chloride ion from the [AuCl(tht)] (tht = tetrahydrothiophene) precursor.

Structure Optimization of the Complexes

Molecular mechanics (MM+ force field) calculations were undertaken with the Spartan'10 program to optimize the minimum-energy geometries of the series of imidazolium salts and the respective mono- and dicarbene derivatives. In particular, our main goal was the analysis of the splitting of the signals of H-4 and H-5 in the ^{1}H NMR spectra. For this, complexes with one, four, and ten methylene groups bonded to the second nitrogen atom were chosen (i.e., MC**1**, MC**4**, MC**5**, DC**1**, DC**4**, and DC**5**).

As expected, the inequivalence of H-4 and H-5 in MC**1** is clearly observed, and the environment becomes more similar for longer substituents (Figure 6, left). On the other hand, on the basis of these models, it is expected that both N-heterocyclic rings in the dicarbene complexes are more distorted from the planar conformation for complexes with shorter alkyl chain lengths (DC**1** and DC**4**), and this hinders the equivalence of the protons (Figure 6, right). On the contrary, the most-stable calculated conformation of DC**5** shows a near-planar disposition of both rings, in agreement with the recorded singlet corresponding to both protons.

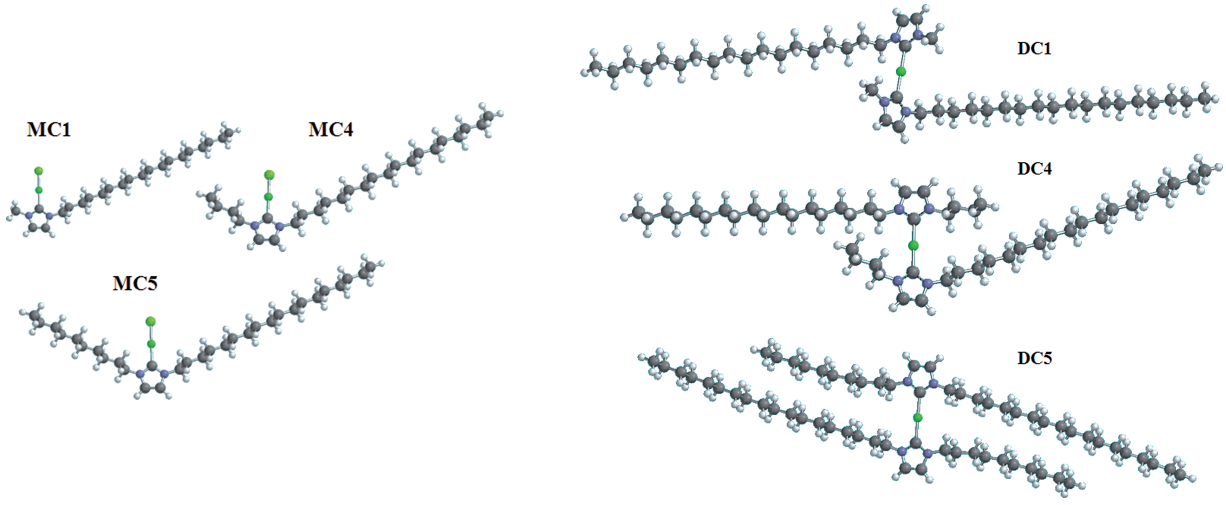

Figure 6. Spartan models of MC**1**, MC**4**, MC**5**, DC**1**, DC**4**, and DC**5**.

Biological Assays

Initially, the effects against tumor cell growth of HT-29 colon carcinoma and MDA-MB-231 breast cancer cells were determined. The results are summarized in Table 1.

Table 1. IC_{50} values [μM] for cytotoxicity in HT-29 and MDA-MB-231 cells and TrxR inhibition [μM]. Mean values of two to four independent experiments with errors in parentheses.

Compound	IC_{50} HT-29	IC_{50} MDA-MB 231	TrxR
1	3.10 (1.38)	1.49 (0.97)	>10
3	3.22 (1.50)	1.28 (0.84)	
4	3.43 (0.39)	1.22 (0.64)	
5	9.52 (0.73)	8.80 (1.65)	
MC**1**	3.08 (0.25)	3.59 (0.25)	0.320 (0.040)
MC**2**	7.33 (2.46)	4.03 (0.15)	
MC**3**	9.79 (0.22)	4.43 (0.23)	
MCi**3**	9.92 (0.27)	5.15 (0.44)	
MC**4**	9.76 (0.19)	6.12 (1.72)	
MC**5**	8.39 (1.80)	4.33 (0.09)	
DC**1**	38.60 (2.76)	9.25 (1.21)	>10
DC**4**	26.12 (10.65)	16.79 (6.96)	
DC**5**	9.08 (1.26)	5.58 (0.72)	

The metal-free imidazolium salt derivatives **1** and **3**–**5** displayed good cytotoxic activity in both cell lines with IC_{50} values in the low micromolar range.

Previous studies of imidazolium-derived ionic liquids showed that toxicity increases as the alkyl chain length increases, owing to their higher lipophilicity.[39–44] In this study, the activity of the ligands is more or less in a similar range with the exception of **5**, which contains the longest alkyl chain but triggers lower cytotoxicity. This difference compared with previously reported data could be attributed to the constant presence of the octadecyl chain in all complexes, which means that the lipophilicity is less affected.

The respective gold chloride analogues MC**1**–MC**5** also exhibited strong antiproliferative effects. However, the activities decreased in most cases compared to those of the imidazolium derivatives. A further loss of cytotoxic potency was observed for the bis-NHC complexes DC**1** and DC**4**, which triggered only very modest cell growth inhibitory effects in both cell lines. It should be noted, however, that the general decrease of cytotoxic activity upon gold(I) coordination was less evident for analogues **5**, MC**5**, and DC**5**, which differ from the other compounds by containing the longest alkyl side chains (C_{18} and C_{10}). In this case, the cytotoxicity values remained in a rather narrow range between 4 and 10 μM.

Overall the results clearly indicate that the inhibition of tumor cell growth is largely driven by the long lipophilic side chains of the compounds and not by the presence of the gold(I) center.

The inhibition of the activity of the enzyme TrxR was evaluated for some selected species. One compound of each series (**1**, MC**1**, and DC**1**) was selected to analyze the effect of the metal atom and the presence of one or two carbene ligands coordinated to the gold center. As can be observed in Table 1, the best results were obtained for the monocarbene complex; this suggests that the metal atom has a role in the inhibition of this enzyme together with the necessary presence of a labile ligand (chloride instead of carbene group). The value for MC**1** is in the same range as the reported values of other gold(I) monocarbene chlorido complexes.[35] Also, as previously reported, the TrxR inhibition of the cationic dicarbene species DC**1** was lower than that of the monocarbene analogue MC**1**, and no IC_{50} value could be calculated up to the highest used concentration of 10 μM.[26] As expected, the gold-free analogue **1** was also inactive.

Conclusions

The synthesis of a series of imidazolium salts from 1-octadecylimidazole by anchoring different alkyl groups (methyl, ethyl, isopropyl, propyl, butyl, decyl and octadecyl) at the second nitrogen atom has been successfully achieved in moderate-to-high yields.

To evaluate the cytotoxicity of their corresponding gold(I) derivatives, two series of complexes (monocarbenes and dicarbenes) were prepared.

The H-4 and H-5 protons become equivalent when both alkyl chains bonded to the nitrogen atoms are long (R = butyl and decyl for monocarbene and R = decyl for dicarbene) owing to the expected conformation of the complexes.

Their biological activity against tumor cell growth of HT-29 colon carcinoma and MDA-MB-231 breast cancer cells demonstrated that the metal-free imidazolium iodide derivatives **1** and **3**–**5** displayed good cytotoxic activity in both cell lines. Moreover, their activity was decreased for **5**, which contains the longest alkyl chain. The cytotoxic activity was in general driven by the lipophilicity of the alkyl chains. The introduction of gold carbene partial structures did not increase the cytotoxic potency. However, for the monocarbene derivative MC**1**, potent TrxR inhibition could be confirmed. This is indicative that the shorter substituent is a key factor for this activity.

Experimental Section

General Procedures: All manipulations were performed under purified N_2 by standard Schlenk techniques. All solvents were distilled from appropriate drying agents. The commercially available reagents CH_3I, CH_3CH_2I, $CH_3(CH_2)_2I$, $CH(CH_3)_2I$, $CH_3(CH_2)_3I$, $CH_3(CH_2)_9I$, and Ag_2O were used as received from Sigma–Aldrich. Literature methods were used to prepare octadecylimidazole (Im18),[34] bis(Im18),[34] and [AuCl(tht)].[45]

Physical Measurements: Infrared spectra were recorded with a Nicolet 520 FTIR Spectrophotometer. ^1H NMR [$\delta(SiMe_4)$ = 0.0 ppm] spectra were obtained with Varian Unity 400 and Varian Inova 300 spectrometers. ES(+) and ES(–) mass spectra were recorded with a Fisons VG Quatro spectrometer. Elemental analyses of C, H, and N were performed at the Centres Científics i Tecnològics Universitat de Barcelona (CCiT-UB) and with a Thermo Quest CE Instruments Flash EA 1112 analyzer at the Institute of Medicinal and Pharmaceutical Chemistry in Braunschweig.

Structure Optimization: Molecular modeling was performed with the software Spartan'10 V1.0.1 for Windows. The structures were previously optimized at the MM+ molecular mechanics level.

1-Methyl-3-octadecylimidazolium Iodide (1): Iodomethane (440 μL, 7.07 mmol) was added to an acetonitrile solution (50 mL) of octadecylimidazole (450 mg, 1.40 mmol). The solution was stirred under reflux for 18 h, and the resulting yellow solution was concentrated under vacuum to 2 mL. A yellow solid was obtained after the addition of diethyl ether (40 mL). The solid was collected by filtration to give **1** in 85% yield (553 mg). IR (KBr): $\tilde{\nu}$ = 3075 (st, =CH–), 2917, 2848 (st, C–H), 1560 (st, N=C) cm^{-1}. ^1H NMR (400.11 MHz, 298 K, $CDCl_3$): δ = 10.45 (s, 1 H, NC*H*N), 7.21 (s, 1 H, NCHC*H*NCH$_3$), 7.19 (s, 1 H, NC*H*CHNCH$_3$), 4.31 (t, $^3J_{H,H}$ = 7.5 Hz, 2 H, CH$_2$C*H*$_2$N), 4.12 (s, 3 H, CH$_3$N), 2.01 1.86 (m, 2 H, C*H*$_2$CH$_2$N), 1.42–1.15 [m, 30 H, CH$_3$(C*H*$_2$)$_{15}$], 0.88 [t, $^3J_{H,H}$ = 6.7 Hz, 3 H, C*H*$_3$(CH$_2$)$_{15}$] ppm. MS (ES+): *m*/*z* = 335.34 $[M]^+$. $C_{22}H_{43}IN_2$ (462.50): calcd. C 57.13, H 9.37, N 6.06; found C 56.98, H 9.32, N 5.89.

1-Ethyl-3-octadecylimidazolium Iodide (2): A similar procedure with iodoethane instead of iodomethane was used to obtain **2**. A white solid was obtained in 40% yield (89 mg). IR (KBr): $\tilde{\nu}$ = 3075 (st, =CH–), 2917, 2848 (st, C–H), 1560 (st, N=C), 1465, 1375 (δ, –CH$_3$, –CH$_2$) cm^{-1}. ^1H NMR (400.11 MHz, 298 K, $CDCl_3$): δ = 10.55 (s, 1 H, NC*H*N), 7.24 (s, 1 H, NCHC*H*NEt), 7.20 (s, 1 H, NC*H*CHNEt), 4.44 (q, $^3J_{H,H}$ = 7.4 Hz, 2 H, NC*H*$_2$CH$_3$), 4.34 (t, $^3J_{H,H}$ = 7.5 Hz, 2 H, CH$_2$C*H*$_2$N), 1.99–1.88 (m, 2 H, C*H*$_2$CH$_2$N), 1.64 (t, $^3J_{H,H}$ = 7.4 Hz, 3 H, NCH$_2$C*H*$_3$), 1.39–1.19 [m, 30 H, CH$_3$(C*H*$_2$)$_{15}$], 0.88 [t, $^3J_{H,H}$ = 6.7 Hz, 3 H, C*H*$_3$(CH$_2$)$_{15}$] ppm. MS (ES+): *m*/*z* = 349.35 $[M]^+$. $C_{23}H_{45}IN_2$ (476.53): calcd. C 57.97, H 9.52, N 5.88; found C 57.90, H 9.48, N 5.81.

1-Propyl-3-octadecylimidazolium Iodide (3): A similar procedure with 1-iodopropane instead of iodomethane was used to obtain **3**. Yellow solid (yield: 190 mg, 82%). IR (KBr): $\tilde{\nu}$ = 3075 (st, =CH–), 2917, 2848 (st, C–H), 1560 (st, N=C), 1465, 1375 (δ, –CH$_3$, –CH$_2$) cm^{-1}. ^1H NMR (400.11 MHz, 298 K, $CDCl_3$): δ = 10.56 (s, 1 H, NC*H*N), 7.20 (s, 2 H, NC*HCH*N), 4.40–4.27 (m, 4 H, CH$_2$C*H*$_2$N), 2.07–1.84 (m, 4 H, C*H*$_2$CH$_2$N), 1.44–1.14 [m, 30 H, CH$_3$(C*H*$_2$)$_{15}$], 1.02 (t, $^3J_{H,H}$ = 7.4 Hz, 3 H, C*H*$_3$CH$_2$CH$_2$N), 0.88 [t, $^3J_{H,H}$ = 6.7 Hz, 3 H, C*H*$_3$(CH$_2$)$_{15}$] ppm. MS: (ES+) *m*/*z* = 363.38 $[M]^+$. $C_{24}H_{47}IN_2$ (490.55): calcd. C 58.76, H 9.66, N 5.71; found C 58.70, H 9.59, N 5.65.

1-Isopropyl-3-octadecylimidazolium Iodide (i3): A similar procedure with 2-iodopropane instead of iodomethane was used to obtain i**3**. Yellow solid (yield: 109 mg, 47%). IR (KBr): $\tilde{\nu}$ = 3075 (st, =CH–), 2917, 2848 (st, C–H), 1560 (st, N=C), 1465, 1375 (δ, –CH$_3$, –CH$_2$) cm^{-1}. ^1H NMR (400.11 MHz, 298 K, $CDCl_3$): δ = 10.63 (s, 1 H, NC*H*N), 7.23 (s, 1 H, NCHC*H*N*i*Pr), 7.18 (s, 1 H, NC*H*CHN*i*Pr), 4.92 [hept, $^3J_{H,H}$ = 6.7 Hz, 1 H, C*H*(CH$_3$)$_2$], 4.38 (t, $^3J_{H,H}$ = 7.5 Hz, 2 H, CH$_2$C*H*$_2$N), 2.00–1.88 (m, 2 H, C*H*$_2$CH$_2$N), 1.66 [d, $^3J_{H,H}$ = 6.7 Hz, 6 H, CH(C*H*$_3$)$_2$], 1.41–1.14 [m, 30 H, CH$_3$(C*H*$_2$)$_{15}$], 0.88 [t, $^3J_{H,H}$ = 6.7 Hz, 3 H, C*H*$_3$(CH$_2$)$_{15}$] ppm. MS (ES+): *m*/*z* = 363.38 $[M]^+$. $C_{24}H_{47}IN_2$ (490.55): calcd. C 58.76, H 9.66, N 5.71; found C 58.69, H 9.58, N 5.67.

1-Butyl-3-octadecylimidazolium Iodide (4): A similar procedure with 1-iodobutane instead of iodomethane was used to obtain **4**. Yellow solid (yield: 183 mg, 77%). IR (KBr): $\tilde{\nu}$ = 3075 (st, =CH–), 2917, 2848 (st, C–H), 1560 (st, N=C) cm^{-1}. ^1H NMR (400.11 MHz, 298 K, $CDCl_3$): δ = 10.58 (s, 1 H, NC*H*N), 7.18 (s, 2 H, NC*HCH*N), 4.41–4.28 (m, 4 H, CH$_2$C*H*$_2$N), 1.99–1.86 (m, 4 H, C*H*$_2$CH$_2$N), 1.47–1.12 [m, 32 H, CH$_3$(C*H*$_2$)$_{15}$ + CH$_3$C*H*$_2$(CH$_2$)$_2$N], 0.99 [t, $^3J_{H,H}$ = 7.4 Hz, 3 H, C*H*$_3$CH$_2$(CH$_2$)$_2$N], 0.88 [t, $^3J_{H,H}$ = 6.7 Hz, 3 H, C*H*$_3$(CH$_2$)$_{15}$] ppm. MS (ES+): *m*/*z* = 377.39 $[M]^+$. $C_{25}H_{49}IN_2$ (504.58): calcd. C 59.51, H 9.79, N 5.55; found C 59.55, H 9.94, N 5.32.

1-Decyl-3-octadecylimidazolium Iodide (5): A similar procedure with 1-iododecane instead of iodomethane was used to obtain **5**. White solid (yield: 326 mg, 88%). IR (KBr): $\tilde{\nu}$ = 3075 (st, =CH–), 2917, 2848 (st, C–H), 1560 (st, N=C) cm^{-1}. ^1H NMR (400.11 MHz, 298 K, $CDCl_3$): δ = 10.62 (s, 1 H, NC*H*N), 7.16 (d, $^3J_{H,H}$ = 1.3 Hz, 2 H, NC*HCH*N), 4.35 (t, $^3J_{H,H}$ = 7.5 Hz, 4 H, CH$_2$C*H*$_2$N), 1.98–1.88 (m, 4 H, C*H*$_2$CH$_2$N), 1.42–1.19 [m, 44 H, CH$_3$(C*H*$_2$)$_{15}$, CH$_3$(C*H*$_2$)$_7$(CH$_2$)$_2$N], 0.88 [t, $^3J_{H,H}$ = 6.7 Hz, 6 H, C*H*$_3$(CH$_2$)$_{15}$, C*H*$_3$(CH$_2$)$_9$N] ppm. MS (ES+): *m*/*z* = 461.49 $[M]^+$. $C_{31}H_{61}IN_2$ (588.74): calcd. C 63.24, H 10.44, N 4.76; found C 63.58, H 10.41, N 4.54.

[(1)AuCl] (MC1): A dichloromethane solution (60 mL) of **1** (500 mg. 1.08 mmol) and Ag_2O (125 mg, 0.54 mmol) was stirred for 5 h at room temperature protected from light with aluminum foil. [AuCl(tht)] (346 mg, 1.08 mmol) was added as a solid. After 15 h of stirring, the solution was filtered through Celite, and the resulting yellow solution was concentrated to dryness to obtain an orange solid. Yield: 525 mg, 86%. IR (KBr): $\tilde{\nu}$ = 3092 (st, =CH–), 2917, 2848 (st, C–H), 1560 (st, N=C) cm^{-1}. ^1H NMR (400.11 MHz, 298 K, $CDCl_3$): δ = 6.93–6.90 (m, 2 H, NC*HCH*N), 4.14 (t, $^3J_{H,H}$ = 7.3 Hz, 2 H, CH$_2$C*H*$_2$N), 3.83 (s, 3 H, C*H*$_3$N), 1.90–1.70 (m, 2 H, C*H*$_2$CH$_2$N), 1.36–1.12 [m, 30 H, CH$_3$(C*H*$_2$)$_{15}$], 0.88 [t, $^3J_{H,H}$ = 6.8 Hz, 3 H, C*H*$_3$(CH$_2$)$_{15}$] ppm. MS (ES+): *m*/*z* = 572.32 [M – Cl + MeCN]$^+$, 321.33 [Im18 + H]$^+$. $C_{22}H_{42}AuClN_2$ (567.01): calcd. C 46.60, H 7.47, N 4.94; found C 46.53, H 7.40, N 4.89.

[(2)AuCl] (MC2): The procedure for the synthesis of MC**1** was applied for MC**2**, but **2** was used instead of **1**. A brown solid was obtained in 26% yield (51 mg). IR (KBr): $\tilde{\nu}$ = 3092 (st, =CH–), 2917, 2848 (st, C–H), 1560 (st, N=C) cm^{-1}. ^1H NMR (400.11 MHz, 298 K, $CDCl_3$): δ = 6.96–6.91 (m, 2 H, NC*HCH*N), 4.23 (q, $^3J_{H,H}$ = 7.4 Hz, 2 H, CH$_3$C*H*$_2$N), 4.17–4.11 (m, 2 H, CH$_2$C*H*$_2$N), 1.89–1.76 (m, 2 H, C*H*$_2$CH$_2$N), 1.47 (t, $^3J_{H,H}$ = 7.4 Hz, 3 H, C*H*$_3$CH$_2$N), 1.37–1.18 [m, 30 H, CH$_3$(C*H*$_2$)$_{15}$], 0.88 [t, $^3J_{H,H}$ = 6.6 Hz, 3 H, C*H*$_3$(CH$_2$)$_{15}$] ppm. MS (ES+): *m*/*z* = 586.34 [M – Cl + MeCN]$^+$, 545.32 [M – Cl]$^+$, 321.33 [Im18 + H]$^+$. $C_{23}H_{44}AuClN_2$ (581.03): calcd. C 47.54, H 7.63, N 4.82; found C 47.49, H 7.50, N 4.75.

[(3)AuCl] (MC3): The procedure for the synthesis of MC**1** was applied for MC**3**, but **3** was used instead of **1**. A yellow solid was obtained in 6% yield (13 mg). IR (KBr): $\tilde{\nu}$ = 3092 (st, =CH–), 2917, 2848 (st, C–H), 1560 (st, N=C) cm^{-1}. ^1H NMR (400.11 MHz, 298 K, $CDCl_3$): δ = 6.92 (d, $^3J_{H,H}$ = 2.1 Hz, 2 H, NC*HCH*N), 4.23–4.00 (m, 4 H, CH$_3$C*H*$_2$N, CH$_2$C*H*$_2$N), 1.98–1.72 (m, 4 H, C*H*$_2$CH$_2$N, CH$_3$C*H*$_2$CH$_2$N), 1.38–1.13 [m, 30 H, CH$_3$(C*H*$_2$)$_{15}$], 0.95 (t, $^3J_{H,H}$ = 7.4 Hz, 3 H, C*H*$_3$CH$_2$CH$_2$N), 0.88 [t, $^3J_{H,H}$ = 6.6 Hz, 3 H, C*H*$_3$(CH$_2$)$_{15}$] ppm. MS (ES+): *m*/*z* = 600.36 [M – Cl + MeCN]$^+$, 559.33 [M – Cl]$^+$, 321.33 [Im18 + H]$^+$. $C_{24}H_{46}AuClN_2$ (595.06): calcd. C 48.44, H 7.79, N 4.71; found C 48.14, H 7.76, N 4.42.

[(i3)AuCl] (MCi3): The procedure for the synthesis of MC**1** was applied for MCi**3**, but i**3** was used instead of **1**. A white solid was obtained in 43% yield (46 mg). IR (KBr): $\tilde{\nu}$ = 3092 (st, =CH–), 2917, 2848 (st, C–H), 1560 (st, N=C) cm^{-1}. ^1H NMR (400.11 MHz, 298 K, $CDCl_3$): δ = 6.99–6.91 (m, 2 H, NC*HCH*N), 5.12–5.00 [m, 1 H, (CH$_3$)$_2$C*H*N], 4.13 (t, $^3J_{H,H}$ = 7.4 Hz, 2 H, CH$_2$C*H*$_2$N), 1.90–1.75 (m, 2 H, C*H*$_2$CH$_2$N), 1.47 [d, $^3J_{H,H}$ = 6.8 Hz, (C*H*$_3$)$_2$CHN], 1.37–1.10 [m, 30 H, CH$_3$(C*H*$_2$)$_{15}$], 0.88 [t, $^3J_{H,H}$ = 6.7 Hz, 3 H, C*H*$_3$(CH$_2$)$_{15}$] ppm. MS (ES+): *m*/*z* = 600.36 [M – Cl + MeCN]$^+$, 559.33 [M – Cl]$^+$, 321.33 [Im18 + H]$^+$. $C_{24}H_{46}AuClN_2$ (595.06): calcd. C 48.44, H 7.79, N 4.71; found C 48.36, H 7.72, N 4.69.

[(4)AuCl] (MC4): The procedure for the synthesis of MC**1** was applied for MC**4**, but **4** was used instead of **1**. The orange solid obtained was sonicated with hexane to obtain a yellow solid in 75%

yield (271 mg). IR (KBr): $\tilde{\nu}$ = 3092 (st, =CH–), 2917, 2848 (st, C–H), 1560 (st, N=C) cm^{-1}. ^{1}H NMR (400.11 MHz, 298 K, $CDCl_3$): δ = 6.92 (s, 2 H, NC*H*C*H*N), 4.21–4.06 [m, 4 H, $CH_3(CH_2)_2CH_2N$, CH_2CH_2N], 1.89–1.75 (m, 4 H, CH_2CH_2N), 1.44–1.16 [m, 32 H, $CH_3(CH_2)_{15}$, $CH_2(CH_2)_2N$], 0.95 [t, $^3J_{H,H}$ = 7.4 Hz, 3 H, $CH_3(CH_2)_3N$], 0.88 [t, $^3J_{H,H}$ = 6.7 Hz, 3 H, $CH_3(CH_2)_{15}$] ppm. MS (ES+): *m*/*z* = 600.36 [M – Cl + MeCN]$^+$, 559.33 [M – Cl]$^+$, 321.33 [Im18 + H]$^+$. $C_{25}H_{48}AuClN_2$ (609.09): calcd. C 49.30, H 7.94, N 4.60; found C 49.24, H 7.73, N 4.55.

[(5)AuCl] (MC5): The procedure for the synthesis of MC**1** was applied for MC**5**, but **5** was used instead of **1**. The resulting oil was purified by column chromatography with dichloromethane as the eluent. An orange solid was obtained in 88% yield (326 mg). IR (KBr): $\tilde{\nu}$ = 3092 (st, =CH–), 2917, 2848 (st, C–H), 1560 (st, N=C) cm^{-1}. ^{1}H NMR (400.11 MHz, 298 K, $CDCl_3$): δ = 6.91 (s, 2 H, NC*H*C*H*N), 4.15 [t, 4 H, $CH_3(CH_2)_8CH_2N$, $CH_3(CH_2)_{16}CH_2N$], 1.92–1.72 [m, 4 H, $CH_3(CH_2)_{15}CH_2CH_2N$, $CH_3(CH_2)_7CH_2CH_2N$], 1.38–1.13 [m, 44 H, $CH_3(CH_2)_{15}$, $CH_3(CH_2)_7(CH_2)_2N$], 0.88 [t, $^3J_{H,H}$ = 6.9 Hz, 6 H, $CH_3(CH_2)_{15}$, $CH_3(CH_2)_9$] ppm. MS (ES+): *m*/*z* = 698.48 [M – Cl + MeCN]$^+$, 657.45 [M – Cl]$^+$, 321.33 [Im18 + H]$^+$. $C_{31}H_{60}AuClN_2$ (693.25): calcd. C 53.71, H 8.72, N 4.04; found C 52.69, H 8.61, N 3.98.

[(1)$_2$Au]I (DC1): Methanol (4 mL) was added to a dichloromethane solution (4 mL) of MC**1** (90 mg. 0.16 mmol), **1** (73 mg, 0.16 mmol), and K_2CO_3 (22 mg, 0.16 mmol), and the solution was stirred for 18 h at room temperature protected from light with aluminum foil. The resulting suspension was concentrated to dryness, extracted with CH_2Cl_2 (10 mL), and precipitated with diethyl ether (10 mL). A white solid was obtained in 52% yield (82 mg). IR (KBr): $\tilde{\nu}$ = 3075 (st, =CH–), 2917, 2848 (st, C–H), 1560 (st, N=C) cm^{-1}. ^{1}H NMR (400.11 MHz, 298 K, $CDCl_3$): δ = 7.20 (d, $^3J_{H,H}$ = 1.8 Hz, 2 H, NCHC*H*NCH$_3$), 7.10 (d, $^3J_{H,H}$ = 1.8 Hz, 2 H, NC*H*CHNCH$_3$), 4.21 [t, $^3J_{H,H}$ = 7.2 Hz, 4 H, $CH_3(CH_2)_{15}CH_2N$], 3.99 (s, 6 H, CH_3N), 1.95–1.80 (m, 4 H, CH_2CH_2N), 1.40–1.12 [m, 60 H, $CH_3(CH_2)_{15}$], 0.88 [t, $^3J_{H,H}$ = 6.8 Hz, 6 H, $CH_3(CH_2)_{15}$] ppm. MS (ES+): *m*/*z* = 865.63 [(**1**)$_2$Au]$^+$, 321.33 [Im18 + H]$^+$. $C_{44}H_{86}AuIN_4$ (995.06): calcd. C 53.11, H 8.71, N 5.63; found C 52.96, H 8.67, N 5.42.

[(4)$_2$Au]I (DC4): The procedure for the synthesis of DC**1** was applied for DC**4**, but MC**4** and **4** were used instead of MC**1** and **1**. An orange solid was obtained in 22% yield (39 mg) after purification by column chromatography (CH_2Cl_2/MeOH, 95:5). IR (KBr): $\tilde{\nu}$ = 3075 (st, =CH–), 2917, 2848 (st, C–H), 1560 (st, N=C) cm^{-1}. ^{1}H NMR (400.11 MHz, 298 K, $CDCl_3$): δ = 7.23 (d, $^3J_{H,H}$ = 1.9 Hz, 2 H, NCHC*H*NBu), 7.21 (d, $^3J_{H,H}$ = 1.9 Hz, 2 H, NC*H*CHNBu), 4.29–4.16 (m, 8 H, CH_2CH_2N), 1.95–1.80 (m, 8 H, CH_2CH_2N), 1.46–1.15 [m, 64 H, $CH_3(CH_2)_{15}$, $NCH_2CH_2CH_2CH_3$], 0.95 (t, $^3J_{H,H}$ = 7.4 Hz, 6 H, $NCH_2CH_2CH_2CH_3$), 0.88 [t, $^3J_{H,H}$ = 6.9 Hz, 6 H, $CH_3(CH_2)_{15}$] ppm. MS (ES+): *m*/*z* = 949.73 [(**4**)$_2$Au]$^+$, 321.33 [Im18 + H]$^+$. $C_{50}H_{96}AuIN_4$ (1077.21): calcd. C 55.75, H 8.98, N 5.20; found C 55.93, H 9.12, N 5.12.

[(5)$_2$Au]Cl (DC5): The procedure for the synthesis of DC**1** was applied for DC**5**, but MC**5** and **5** were used instead of MC**1** and **1**. A white solid was obtained in 38% yield (35 mg). IR (KBr): $\tilde{\nu}$ = 3075 (st, =CH–), 2917, 2848 (st, C–H), 1560 (st, N=C) cm^{-1}. ^{1}H NMR (400.11 MHz, 298 K, $CDCl_3$): δ = 7.22 (s, 4 H, NC*H*C*H*N), 4.23 (t, $^3J_{H,H}$ = 8.1 Hz, 8 H, CH_2CH_2N), 1.95–1.78 (m, 8 H, CH_2CH_2N), 1.43–1.14 [m, 88 H, $CH_3(CH_2)_{15}$, $CH_3(CH_2)_7(CH_2)_2N$], 0.96 [t, $^3J_{H,H}$ = 7.4 Hz, 6 H, $CH_3(CH_2)_{15}$], 0.94–0.77 [m, 12 H, $CH_3(CH_2)_{15}$, $CH_3(CH_2)_9$] ppm. MS (ES+): *m*/*z* = 1117.92 [M]$^+$, 321.33 [Im18 + H]$^+$. $C_{62}H_{122}AuIN_4$ (1247.54): calcd. C 66.45, H 10.97, N 5.00; found C 66.67, H 11.06, N 4.89.

TrxR Inhibition Assay: To determine the inhibition of TrxR, an established microplate-reader-based assay was performed with minor modifications.[26] For this purpose, commercially available recombinant rat liver TrxR 1 (from IMCO Corporation Ltd AB) was used and diluted with distilled water to achieve a concentration of 0.05 U/mL. The compounds were freshly dissolved as stock solutions in *N*,*N*-dimethylformamide (DMF). To each 25 μL aliquot of the enzyme solution, potassium phosphate buffer (pH 7.0, 25 μL) containing the compounds in graded concentrations or vehicle (DMF) without compounds (control probe) was added, and the resulting solutions (final concentration of DMF: max. 0.5% v/v) were incubated with moderate shaking for 75 min at 37 °C in a 96-well plate. The reaction mixture [225 μL; 1000 μL of reaction mixture consisted of 500 μL of potassium phosphate buffer pH 7.0, 80 μL of 100 mM ethylenediaminetetraacetic acid (EDTA) solution at pH 7.5, 20 μL of bovine serum albumin (BSA) solution 0.2%, 100 μL of 20 mM nicotinamide adenine dinucleotide phosphate (NADPH) solution, and 300 μL of distilled water] were added to each well, and the reaction was started by the addition of a 20 mM ethanolic dithio(bis-2-nitrobenzoic acid) (DTNB) solution (25 μL). After proper mixing, the formation of 5-thio-2-nitrobenzoic acid (5-TNB) was monitored with a microplate reader (Perkin–Elmer Victor X4) at 405 nm in 35 s intervals for 350 s. For each tested compound, the noninterference with the assay components was confirmed by a negative control experiment with an enzyme-free solution. The IC_{50} values were calculated as the concentration of compound that decreased the enzymatic activity of the untreated control by 50% and are given as the mean and error of two to three independent experiments.

Cell Culture and Antiproliferative Effects: MDA-MB-231 breast adenocarcinoma and HT-29 colon carcinoma were maintained in Dulbecco's Modified Eagle's Medium (DMEM) high glucose (PAA) supplemented with gentamycin (50 mg/L) and 10% (v/v) fetal calf serum (FCS) at 37 °C under a 5% CO_2 atmosphere and passaged every 7 d. The antiproliferative effects were determined as described in a recent publication.[26] The antiproliferative effects against MDA-MB-231 cells were determined after 96 h.

Supporting Information (see footnote on the first page of this article): ^{1}H NMR spectra of MC**1**, MC**5**, DC**1**, and DC**5** in $CDCl_3$.

Acknowledgments

The authors are grateful to the Ministerio de Ciencia e Innovación of Spain (Projects CTQ2012-31335 and TEC2011-29140-C03-02) and to the Generalitat de Catalunya (project 2009SGR158). COST Actions CM1005 and CM1105 are also acknowledged.

[1] B. Çetinkaya, P. Dixneuf, M. F. Lappert, *J. Chem. Soc., Dalton Trans.* **1974**, 1827.
[2] M. Marion, S. P. Nolan, *Chem. Soc. Rev.* **2008**, *37*, 1776.
[3] S. P. Nolan, *Acc. Chem. Res.* **2011**, *44*, 91.
[4] M. Poyatos, J. A. Mata, E. Peris, *Chem. Rev.* **2009**, *109*, 3677.
[5] L. Casal-Dujat, M. Rodrigues, A. Yagüe, A. C. Calpena, D. B. Amabilino, J. González-Linares, M. Borràs, L. Pérez-García, *Langmuir* **2012**, *28*, 2368.
[6] P. J. Barnard, S. J. Berners-Price, *Coord. Chem. Rev.* **2007**, *251*, 1889.
[7] L. Mercs, M. Albrecht, *Chem. Soc. Rev.* **2010**, *39*, 1903.
[8] C. Hu, X. Li, W. Wang, R. Zhang, L. Deng, *Curr. Med. Chem.* **2014**, *21*, 1220.
[9] W. Liu, R. Gust, *Chem. Soc. Rev.* **2013**, *42*, 755.

[10] H. G. Raubenheimer, S. Cronje, *Chem. Soc. Rev.* **2008**, *37*, 1998.
[11] A. B. Mullick, Y. M. Chang, I. Ghiviriga, K. A. Abboud, W. Tan, A. S. Veige, *Dalton Trans.* **2013**, *42*, 7440.
[12] L. Oehninger, R. Rubbiani, I. Ott, *Dalton Trans.* **2013**, *42*, 3269.
[13] J. C. Lima, L. Rodriguez, *Chem. Soc. Rev.* **2011**, *40*, 5442.
[14] R. Visbal, M. C. Gimeno, *Chem. Soc. Rev.* **2014**, *43*, 3551.
[15] R. Visbal, J. M. López-de-Luzuriaga, A. Laguna, M. C. Gimeno, *Dalton Trans.* **2014**, *43*, 328.
[16] R. Visbal, I. Ospino, J. M. López-de-Luzuriaga, A. Laguna, M. C. Gimeno, *J. Am. Chem. Soc.* **2013**, *135*, 4712.
[17] L. Rodríguez, C. Lodeiro, J. C. Lima, R. Crehuet, *Inorg. Chem.* **2008**, *47*, 4952.
[18] L. Rodríguez, M. Ferrer, R. Crehuet, J. Anglada, J. C. Lima, *Inorg. Chem.* **2012**, *51*, 7636.
[19] I. Rivilla, B. Pilar Gómez-Emeterio, M. R. Fructos, M. M. Díaz-Requejo, P. J. Pérez, *Organometallics* **2011**, *30*, 2855.
[20] A. Prieto, M. R. Fructos, M. M. Díaz-Requejo, P. J. Pérez, P. Pérez-Galán, N. Delpont, A. M. Echavarren, *Tetrahedron* **2009**, *65*, 1790.
[21] D. Canseco-Gonzalez, A. Petronilho, H. Mueller-Bunz, K. Ohmatsu, T. Ooi, M. Albrecht, *J. Am. Chem. Soc.* **2013**, *135*, 13193.
[22] P. Nösel, L. Nunes dos Santos Comprido, T. Lauterbach, M. Rudolph, F. Rominger, A. S. K. Hashmi, *J. Am. Chem. Soc.* **2013**, *135*, 15662.
[23] C. Obradors, A. M. Echavarren, *Chem. Commun.* **2014**, *50*, 16.
[24] K. R. Barnes, S. J. Lippard, *Met. Ions Biol. Syst.* **2004**, *42*, 143.
[25] J. C. Lima, L. Rodríguez, *Anti-Cancer Agents Med. Chem.* **2011**, *11*, 921.
[26] R. Rubbiani, S. Can, I. Kitanovic, H. Alborzinia, M. Stefanopoulou, M. Kokoschka, S. Monchgesang, W. S. Sheldrick, S. Wolfl, I. Ott, *J. Med. Chem.* **2011**, *54*, 8646.
[27] M. Pellei, V. Gandin, M. Marinelli, C. Marzano, M. Yousufuddin, H. V. Dias, C. Santini, *Inorg. Chem.* **2012**, *51*, 9873.
[28] R. Rubbiani, E. Schuh, A. Meyer, J. Lemke, J. Wimberg, N. Metzler-Nolte, F. Meyer, F. Mohr, I. Ott, *MedChemComm* **2013**, *4*, 942.
[29] A. Citta, E. Schuh, F. Mohr, A. Folda, M. L. Massimino, A. Bindoli, A. Casini, M. P. Rigobello, *Metallomics* **2013**, *5*, 1006.
[30] B. Bertrand, L. Stefan, M. Pirrotta, D. Monchaud, E. Bodio, P. Richard, P. Le Gendre, E. Warmerdam, M. H. de Jager, G. M. M. Groothuis, M. Picquet, A. Casini, *Inorg. Chem.* **2014**, *53*, 2296.
[31] A. Pratesi, C. Gabbiani, E. Michelucci, M. Ginanneschi, A. M. Papini, R. Rubbiani, I. Ott, L. Messori, *J. Inorg. Biochem.* **2014**, *136*, 161.
[32] A. Bindoli, M. P. Rigobello, G. Scutarib, C. Gabbiani, A. Casini, L. Messori, *Coord. Chem. Rev.* **2009**, *253*, 1692.
[33] J. Arcau, V. Andermark, E. Aguiló, A. Gandioso, A. Moro, M. Cetina, J. C. Lima, K. Rissanen, I. Ott, L. Rodríguez, *Dalton Trans.* **2014**, *43*, 4426.
[34] S. Livi, J.-F. Gérard, J. Duchet-Rumeau, *Chem. Commun.* **2011**, *47*, 3589.
[35] R. Rubbiani, I. Kitanovic, H. Alborzinia, S. Can, A. Kitanovic, L. A. Onambele, M. Stefanopoulou, Y. Geldmacher, W. S. Sheldrick, G. Wolber, A. Prokop, S. Wölfl, I. Ott, *J. Med. Chem.* **2010**, *53*, 8608.
[36] G. D. Frey, R. D. Dewhurst, S. Kousar, B. Donnadieu, G. Bertrand, *J. Organomet. Chem.* **2008**, *693*, 1674.
[37] R.-T. Zhuang, W.-J. Lin, R. R. Zhuang, W.-S. Hwang, *Polyhedron* **2013**, *51*, 132.
[38] S. Hameury, P. de Frémont, P.-A. R. Breuil, H. Olivier-Bourbigou, P. Braunstein, *Dalton Trans.* **2014**, *43*, 4700.
[39] Z. Fei, T. J. Geldbach, D. Zhao, P. J. Dyson, *Chem. Eur. J.* **2006**, *12*, 2122.
[40] V. Jaitely, A. Karatas, A. T. Florence, *Int. J. Pharm.* **2008**, *354*, 168.
[41] S. Stolte, M. Matzke, J. Arning, A. Boschen, W. R. Pitner, U. Welz-Biermann, B. Jastorff, J. Ranke, *Green Chem.* **2007**, *9*, 1170.
[42] S. Stolte, J. Arning, U. Bottin-Weber, M. Matzke, F. Stock, K. Thiele, M. Uerdingen, U. Welz-Biermann, B. Jastorff, J. Ranke, *Green Chem.* **2006**, *8*, 621.
[43] S. Watanabe, M. Sonobe, M. Arai, Y. Tazume, T. Matsuo, T. Nakamura, K. Yoshida, *Chem. Commun.* **2002**, 2866.
[44] A. Chaterjee, D. J. Oh, K. M. Kim, K.-S. Youk, K. H. Ahn, *Chem. Asian J.* **2008**, *3*, 1962.
[45] R. Usón, A. Laguna in *Organometallic Syntheses Vol. 3* (Eds.: R. B. King, J. J. Eisch), Elsevier, Amsterdam, **1986**, p. 322.

Received: August 29, 2014
Published Online: November 7, 2014

